© 2019. Published by The Company of Biologists Ltd | Journal of Experimental Biology (2019) 222, jeb204834. doi:10.1242/jeb.204834

RESEARCH ARTICLE

The interaction between suction feeding performance and prey escape response determines feeding success in larval fish

Noam Sommerfeld[1,2] and Roi Holzman[1,2,*]

ABSTRACT

The survival of larval marine fishes during early development depends on their ability to feed before depleting their yolk reserves. Most larval fish capture prey by expanding their mouth, generating a 'suction flow' that draws the prey into it. These larvae dwell in a hydrodynamic environment that impedes their ability to capture even non-evasive prey; however, the marine environment is characterized by an abundance of evasive prey, predominantly copepods. Copepods sense the hydrodynamic disturbance created by approaching predators and perform high-acceleration escape maneuvers. Using a 3D high-speed video system, we characterized the interaction between *Sparus aurata* larvae and prey from a natural zooplankton assemblage that contained evasive prey, and assessed the factors that determine the outcome of these interactions. At 8–33 days post hatching, larvae preferentially attacked large prey that was moving prior to the initialization of the strike; however, feeding success was lower for larger, more evasive prey. Thus, larvae were challenged in capturing their preferred prey. Larval feeding success increased with increasing Reynolds numbers, but decreased sharply when the prey performed an escape maneuver. The kinematics of successful strikes resulted in a shorter response time but higher hydrodynamic signature available for the prey, suggesting that strike success in our experiments was determined by brevity rather than stealth: executing a fast strike eliminated a potential escape response by the prey. Our observations of prey selectivity reveal that larval performance, rather than preferences, determines their diet during early development.

KEY WORDS: *Sparus aurata*, Reynolds numbers, Feeding kinematics

INTRODUCTION

The vast majority of marine fishes reproduce by external fertilization, producing small eggs (~1 mm) that drift into the open ocean (Houde, 1987; Cowen and Sponaugle, 2009; Barneche et al., 2018). Following a brief period of development (usually lasting several days, depending on the ambient temperature) larvae hatch from the egg and begin to feed autonomously (Hunter, 1981; Houde, 1987; Cowen and Sponaugle, 2009). After metamorphosis, the larvae settle into their adult habitat, either pelagic or benthic. This strategy is termed the 'bipartite life cycle', which highlights the fact that the planktonic larvae live in a habitat that differs from that of the adults (Hunter, 1981; Houde, 1987; Cowen and Sponaugle, 2009). During the pelagic period, larval diets consist of micro- and macro-zooplankton. Similarly to many adult fishes, larvae feed by closing the distance to their prey, then lunging towards it while opening their mouth and expanding their buccal cavity. The expansion of the mouth generates a flow of water that sucks the prey into the mouth, potentially countering its escape response (Holzman et al., 2015; China et al., 2017).

During the first few weeks of their lives, larvae of marine fishes experience high mortality rates, eradicating >90% of individuals before they reach metamorphosis. Previous research has identified multiple agents of this mortality, including predation, advection to unsuitable habitats, low food availability and disease (Hjort, 1914; Houde, 1987, 2008). However, the hydrodynamic environment in which larvae dwell can also impede their feeding performance, leading to reduced feeding success, low feeding rates and possibly starvation (China and Holzman, 2014; Koch et al., 2018; Yavno and Holzman, 2018). In general, the interaction between a solid (e.g. a prey) and the flow around it (e.g. the suction flow of a feeding fish) can be characterized by the dimensionless Reynolds number (*Re*), depicting the ratio between inertial and viscous forces exerted on the solid particle (Vogel, 1994). Larger objects in faster flows are characterized by a hydrodynamic environment of high *Re* (usually defined as $Re>100$), in which inertial forces dominate and flows can be turbulent. Smaller objects (such as zooplankton) in slower flows (such as the suction flows of larval fish) are characterized by a hydrodynamic regime of low to intermediate *Re* (low *Re* is usually defined as $Re<1$ and intermediate $1<Re<100$). In the intermediate *Re* regime, viscous forces are non-negligible, and the flows can be laminar and reversible. Successful feeding events of *Sparus aurata* larvae on rotifers have been characterized by higher *Re* compared with unsuccessful attempts (China and Holzman, 2014; China et al., 2017). The increase in *Re* has been positively correlated with larval length, and mechanistically attributed to successful larvae expanding their buccal cavity faster (resulting in faster suction flows) and opening their mouth to a larger diameter (China and Holzman, 2014; China et al., 2017). While much is known about the interaction between larval fish and inert prey (Hernández, 2000; Krebs and Turingan, 2003; China and Holzman, 2014; China et al., 2017), this knowledge offers only limited insights into the interaction in nature, in which potential prey species usually possess the ability to sense and respond to approaching predators.

Copepods are often the dominant zooplankton within the pelagic habitat, and an important food source for fish and their larvae. Marine pelagic copepods are highly sensitive to hydrodynamic disturbances, which they perceive via the movement of small sensory setae located on their antennae (Yen et al., 1992; Yen and Strickler, 1996; Fields and Yen, 1997). The setae bend under the shear force that may be generated by the movements of organisms (both predators and prey) near the copepod. Strong shear usually triggers an extremely fast escape response, in which a copepod can

[1]School of Zoology, Faculty of Life Sciences, Tel Aviv University, Tel Aviv 69978, Israel. [2]The Inter-University Institute for Marine Sciences, POB 469, Eilat 88103, Israel.

*Author for correspondence (holzman@tauex.tau.ac.il)

R.H., 0000-0002-2334-2551

Received 9 April 2019; Accepted 29 July 2019

Journal of Experimental Biology (2019) 222, jeb204834. doi:10.1242/jeb.204834

accelerate at ∼300 m s^{-2} to speeds of ∼0.5 m s^{-1} (Buskey and Hartline, 2003; Strickler and Balázsi, 2007). Both sensory and motor abilities of copepods improve over ontogeny, leading to a more efficient escape response. In *Acarcia tonsa* and *Temora longicornis*, adult copepods are ∼6 times more sensitive than the nauplii (Fields and Yen, 1997; Titelman, 2001). Correspondingly, the capture probability of nauplii into an artificial siphon flow decreases sharply as they matured (Fields and Yen, 1997).

It is well established that the ability to capture copepods confers an energetic advantage compared with feeding on other prey types, and that a copepod-based diet increases larval fish survival (Beaugrand et al., 2003; Olivotto et al., 2008; Piccinetti et al., 2014). Stomach content analyses of larval fishes generally reveal a preference for copepods over other prey types, and this preference increases with larval age (Pepin and Penney, 1997; Sabatés and Saiz, 2000; Fulford et al., 2006; Jackson and Lenz, 2016). Such selectivity could result from an ontogenetic shift in larval preferences (i.e. larvae direct more attacks towards copepods as they mature) or from an ontogenetic improvement in larval performance (i.e. larvae experience higher success rates on copepods as they mature), or indeed a combination of both. A computational model that calculated the suction forces exerted on escaping prey, predicted that larval ability to counter the prey's escape force improves dramatically with larval size and age (Yaniv et al., 2014). Accordingly, feeding experiments with clownfish larvae (*Amphiprion ocellaris)* have shown that their diet consists only of copepod nauplii (*Parvocalanus crassirostris*) in the first few days post hatching (dph), and that these larvae transition to a diet based on adult copepods only at ∼9 dph (Jackson and Lenz, 2016). However, the mechanism behind this pattern is still unclear. Additionally, while the vast majority of marine fishes reproduce by releasing small pelagic eggs, and provide no parental care, clownfishes provide parental care for their demersal eggs and their larvae hatch at a relatively large size and developed state (Kavanagh and Alford, 2003; Barneche et al., 2018). Therefore, it is unclear how the performance of *Amphiprion* larvae compares with that of the poorly developed smaller larvae that hatch from pelagic eggs.

Our goal was to characterize the interaction between small pelagic larval fish and potential prey from a natural zooplankton assemblage that contains evasive prey. Specifically, we sought to: (1) determine whether larvae are selective to evasive prey; (2) estimate the variables that affect feeding success on such prey; and (3) characterize the effect of larval morphology and kinematics on the escape response of the prey. We used 8–33 dph *S. aurata* larvae, as these larvae hatch from small pelagic eggs, representing the common strategy among marine fishes. The experimental arena was filmed using two synchronized high-speed cameras in a laboratory setup that allowed 3D tracking of both prey and predator.

MATERIALS AND METHODS

Study organisms

We used larvae of gilthead sea bream (*Sparus aurata* Linnaeus 1758) as our model for larval feeding (Holzman et al., 2015). *S. aurata* is a pelagic spawner, hatching at ∼3.5 mm. Feeding initiates at ∼5 dph at a body length of ∼4 mm. Larvae reach the stage of flexion at ∼21–24 dph, at a length of 7–10 mm, depending on conditions. Larvae were provided by the ARDAG commercial nursery (Eilat, Israel). Throughout the experiments, larvae were kept at 19°C in aerated seawater at a salinity of 35 ppm. Larvae were obtained prior to daily feeding and therefore had been food deprived for >12 h. All experiments were approved by the Institutional Animal Care and Use Committee (IACUC) at the Hebrew University of Jerusalem, overseeing the experiments at the IUI Eilat campus.

We used a natural assemblage of zooplankton as the prey in all experiments. Prey were obtained by towing a zooplankton net from a boat cruising at low speed, or by a swimmer, depending on the seasonal abundance of zooplankton in the coastal waters of the Gulf of Aqaba, Eilat, Israel. Swimmers towed a 1-m-long, 100 µm zooplankton net with a mouth diameter of ∼0.5 m, while the boat towed a longer, 4-m-long net. At the end of the tow, the captured zooplankton were sieved through a 500 µm net to remove larger zooplankton, including predatory arrow worms and other elongate organisms, and carefully transferred into a 1 liter holding aerated container until the onset of experiments. A subsample was observed under a stereoscopic microscope to verify that the sample was dominated by copepods; if not, a new sample was obtained. Fresh zooplankton was collected daily for the experiments. Neither collection method (net towed by boat or swimmer) nor season had a significant effect on larval feeding success rates (logistic regression, $P>0.1$ for both); collection method (boat or swimmer) also had no significant effect ($P>0.05$) on the proportion of copepods (mean± 95% CI of 34.5±8.6% and 31.0±3.2% for boat and swimmer, respectively), copepod nauplii (29.6±16.6% and 21.5±4.2%), gastropods (21.5±13.1% and 20.2±4.9%) and bivalves (11.2± 3.2% and 15.7±5.9%); and, finally, collection method (boat or swimmer) had no significant effect on the length of the prey at which strikes were directed ($P>0.1$, 0.42±0.26 and 0.48±0.16 mm, respectively; see below).

3D filming of prey acquisition strikes

We tracked the 3D position of the larvae and their prey during prey acquisition strikes using two synchronized high-speed cameras (Photron Fastcam SA6) operating at 1000 frames per second. Cameras were fitted with Navitar 6000 ultra-zoom lenses, providing 1:3.25 magnification (i.e. a 1-mm-long object is projected as 3.25 mm on the sensor) with a depth of field of ∼50 mm (Fig. 1A). Cameras were positioned such that their resolution and magnification were identical. The field of view of each camera was ∼40 mm×30 mm (width×height) at a resolution of 1920×1440 pixels. The cameras were positioned 45 cm apart, at a relative angle of 35 deg (Fig. 1A). The volume on which the two cameras were focused was ∼20 ml. To minimize reflections and distortions and maximize the depth of field, the aquarium was constructed such that each face was perpendicular to one camera. Two rectangular 2.2 W LED lights were positioned behind the aquarium, providing a backlight illumination of the visualized volume. Light intensity in the aquarium was measured using a Licor LI-250A light meter, and found to range from 90 to 145 µmol m^{-2} s^{-1}, depending on the direction of the probe. This range is equivalent to the light intensity at a depth of ∼20–60 m (depending on season) at our study site around noon time (Dishon et al., 2012). Larvae are visual predators and the majority of larvae in our study site are found at this depth range during the day (Kimmerling et al., 2018). Reconstruction of points in the 3D space was done using the package DLTdv5 in MATLAB (Hedrick, 2008). The system was calibrated at the beginning of each recording session using a calibration grid of 60 points, spanning the visualized volume. Accuracy was assessed by measuring four known distances in three different images, and estimated as <1.5%.

For each filming session, 5–15 larvae were introduced into the filming aquarium and given several minutes to acclimate. A random assortment of prey was then sampled from the holding container

Journal of Experimental Biology (2019) 222, jeb204834. doi:10.1242/jeb.204834

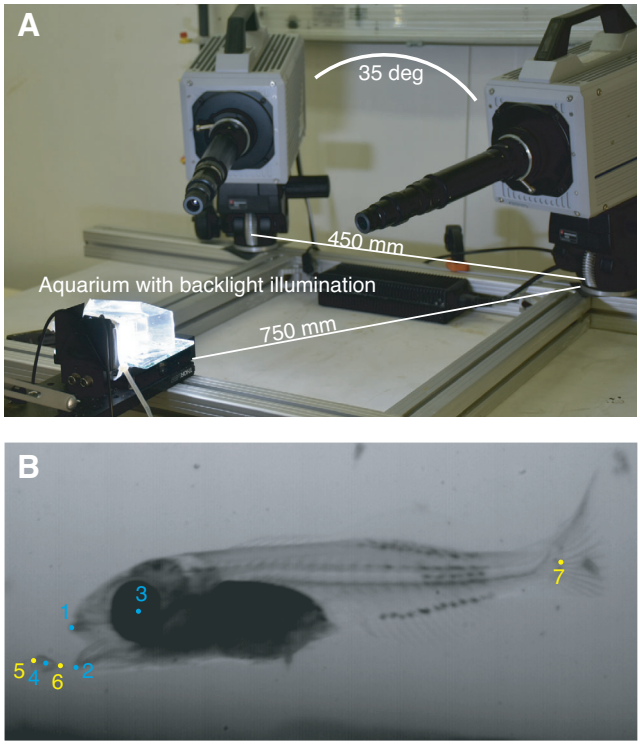

Fig. 1. Experimental setup to film interactions between *Sparus aurata* larvae and their prey. (A) The positions of the larvae and their prey were tracked in 3D using two synchronized Photron Fastcam SA6 high-speed cameras fitted with Navitar 6000 ultra-zoom lenses. The lenses provided 1:3.25 magnification with a depth of field of ∼50 mm. Data were collected at 1000 frames s^{-1} (see Movie 1). (B) Four landmarks (blue dots) were digitized frame-by-frame during the strikes: the anterior tip of the upper (1) and lower jaw (2), the center of the eye (3), and the prey's approximate center of mass (4). Three additional landmarks (yellow) were digitized in one of the frames: the two vertices on the horizontal major axis of an imaginary ellipse encapsulating the prey (5 and 6) and the base of the larva's caudal fin (7).

with a pipette and introduced into the chamber. Larvae were then allowed to feed freely for ∼30 min. Inspection of the videos showed that introduced prey mostly comprised copepods and their nauplii, likely because the other frequent taxa (bivalves and gastropods) sank to the bottom of the holding container. The system was triggered manually upon the observer's detection of a predator's feeding attempt or a prey's escape response in the visualized volume. Thus, our dataset comprised clips that featured: (1) predatory strikes in which the prey initiated an escape response; (2) predatory strikes in which the prey did not move; and (3) escape responses executed by the prey before the predator opened its mouth. For each strike, the time of strike initiation (t=0) was defined as the time at which the prey started to escape (cases 1 and 3 above) or as the time when the larva opened its mouth (case 2). Note that these times were highly correlated (r=0.75) in case 1. Overall, these events involved 100 strikes from larvae ranging in age from 8 to 33 dph (standard length: 3–20 mm). All of the events that were digitized are included in the analysis. Reconstruction of points in the 3D space was done using the package DLTdv5 in MATLAB (Hedrick, 2008). The system was calibrated at the beginning of each recording session using a calibration grid of 60 points, spanning the visualized volume. Accuracy was assessed by measuring four known distances in three different images, and estimated as <1.5%.

For the two views of each recorded event (from each of the two cameras) four landmarks were digitized in each frame (Fig. 1B): (1) the anterior tip of the upper jaw, (2) the anterior tip of the lower jaw, (3) a point on the body (center of the eye) and (4) the prey's approximate center of mass. Three additional landmarks were digitized in one of the frames: the two vertices on the horizontal major axis of an imaginary ellipse encapsulating the prey (5 and 6) and the base of the caudal fin (7; Fig. 1B). Digitized 2D coordinates of the landmarks from the paired cameras were converted to an earthbound 3D coordinate system using DLTdv5. We used the coordinates of the landmarks to calculate the following variables: (1) larval length, calculated as the distance between the center of the mouth to the base of the caudal fin; (2) mouth gape (mm; hereafter 'gape'), calculated at each point in time as the distance between the anterior tip of the upper and lower jaw; (3) time to peak gape (TTPG; ms), calculated as the time it took the larva to open its mouth to 95% of maximal gape diameter; (4) gape opening speed (mm s^{-1}), calculated as the derivative of gape diameter with time; (5) response distance (mm), the distance of the prey from mouth center at the time of strike initiation; (6) larval swimming speed (mm s^{-1}) calculated as the average speed of the larva during the feeding attempt; (7) the time to prey capture (ms); (8) prey cruising speed (mm s^{-1}), calculated based on the displacement of the prey 10 frames before the predator's strike (of prey escape) was initiated; (9) prey escape speed (mm s^{-1}), calculated based on the displacement of the prey during its escape, usually <10 frames; and (10) prey length (mm). We used these values to calculate the Reynolds number (Eqn 1) for feeding and swimming of the larvae. *Re* was calculated as:

$$Re = \frac{\rho l U}{\mu}, \quad (1)$$

where ρ is the density (1024 kg m^{-3}) and μ is the dynamic viscosity (Pa s^{-1}) of the fluid. Re_{feeding} was calculated using maximal gape diameter as the relevant length (l; m) and the peak suction flow speed (U; m s^{-1}). The latter speed was estimated based on TTPG, maximal gape, and estimated buccal dimensions (Yaniv et al., 2014; China et al., 2017). Re_{swimming} was calculated using the larva's length as the relevant length (l; m), and its swimming speed as the flow velocity (U; m s^{-1}).

Determinants of feeding success

We used logistic regression to estimate the effects of kinematic and morphological traits of both prey and predator on feeding success. The dependent variable was larval feeding success (fail vs success; binary variable). The independent variables were selected following China et al. (2017), who found that the variance in feeding success on non-evasive prey was explained only by the hydrodynamic environment (*Re*). Because our prey was evasive, we also included variables that can affect the prey's performance, i.e. whether it initiated an escape response (yes/no; binary variable), prey length, response distance, and prey swimming speed (before the strike was initiated). We used a model-averaging approach to identify and weight the variables that affect feeding success. We used the function dredge in R (https://cran.r-project.org/web/packages/MuMIn/index.html) to identify the best supported models (with ΔAIC<2 relative to the best model), followed by calculation of model averaged estimates of the effect size and standard error for each variable (Vonta, 2010).

Journal of Experimental Biology (2019) 222, jeb204834. doi:10.1242/jeb.204834

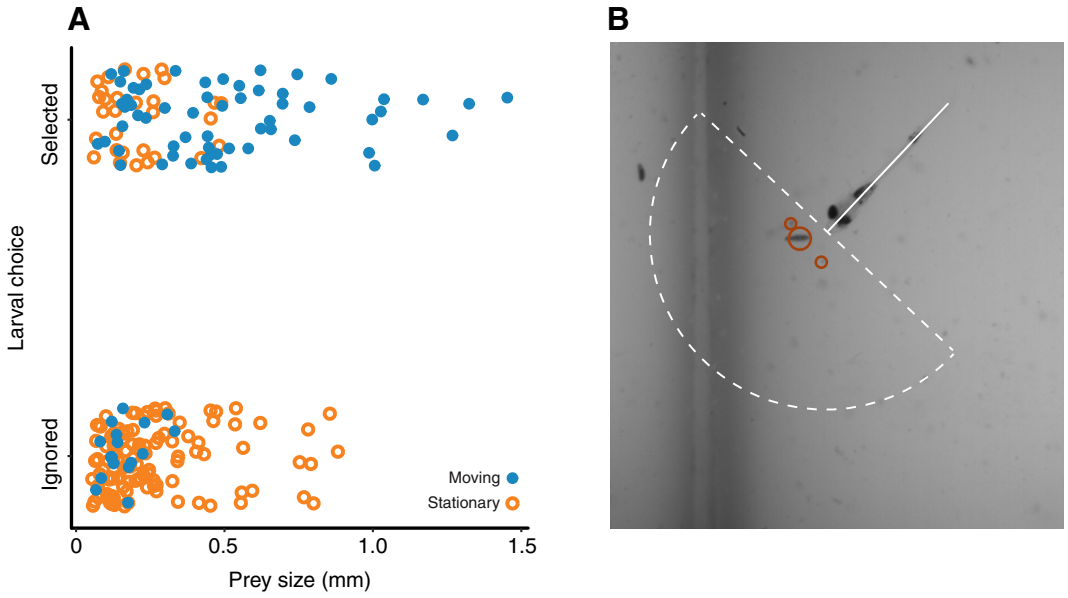

Fig. 2. *Sparus aurata* larvae tend to strike larger, moving prey. (A) Point colors depict whether the prey was stationary (orange) or moving (blue) in the 10 frames preceding the strike. (B) Data in A refer to all zooplankton (circled in red) located within an imaginary hemisphere (white dashed shape), with a diameter of 1 larval body length, centered at the larva's mouth. *N*=90 strikes and 223 prey items. See also Table 1.

We used a logistic regression model to test which variables determined the prey's escape response. Copepods are known to execute an escape response when exposed to high strain rates. These can be caused by the body of the approaching predator, in which case the disturbance is expected to increase with the swimming speed of the predator, the radius of the fish's head, and the distance between the predator and prey. Kiørboe (2008) estimated this disturbance (γ; s^{-1}) as:

$$\gamma = \frac{3(2a^2Rv + aR^2v)}{2(a+R)^2}, \quad (2)$$

where R is the distance between the anterior end of the larvae and the prey (m), a is the radius of the larva's head (m), and ν is the swimming speed of the larvae ($m\,s^{-1}$). Our model therefore included prey length, larval swimming speed, the radius of the larva's head, and strike initiation distance as independent variable, and prey escape as a binary dependent variable.

Selectivity

We characterized the prey available to the larvae before each strike by measuring the length and tracking the motion of all potential prey items located within the larvae's reactive volume. That volume was defined as a hemisphere with a diameter of 1 larval body length, centered at the larva's mouth, and with the plane passing through the center of the hemisphere perpendicular to the larva's long axis (Fig. 2). We used only strikes in which the reactive volume contained more than one prey (*N*=90). We tested the effect of the length (mm) and motion (binary variable: moving/stationary) on the probability of a larva striking a prey item using conditional logistic regression. In this analysis, each strike was considered a choice experiment, incorporated into the model as a stratum (i.e. random variable; Aizaki and Nishimura, 2008).

Table 1. Conditional logistic regression model depicting the effect of prey length (mm) and motion (binary variable: moving/stationary) on the probability of a fish attempting to capture it

	Estimate	s.e.	*Z* value	*P*
Size	4.07	1.50	2.71	0.007
Motion	2.17	0.43	5.05	0.0001

Model R^2=0.26; s.e., adjusted standard error of the estimate. *N*=90 strikes and 223 prey items.

RESULTS

Selectivity

In all strikes in which more than one prey was present at a distance of 1 larval length, attacks were directed towards the larger, moving prey (conditional logistic regression; $P<0.001$ for size and $P<0.007$ for movement; whole model R^2=0.26, $P<0.001$; *N*=90 strikes and 223 prey items; Fig. 2; Table 1). The logistic regression indicated that a 1 mm increase in the size of the prey would increase attack probability four-fold and that prey movement would double attack probability (Table 1). Accordingly, the size of attacked prey ranged from 0.06 to 1.5 mm (median 0.36 mm) and that of ignored prey ranged from 0.06 to 0.9 mm (median 0.18). Roughly two-thirds of the attacks were directed at prey that were moving before the strike was initiated (Fig. 2).

Table 2. Conditional averages of effect sizes from the seven best logistic regression models, depicting the effect of independent variables on feeding success

	Estimate	s.e.	*Z* value	*P*	Rank
Intercept	1.31	0.86	1.52	0.127	
Prey escape (Y/N)	–2.04	0.77	2.66	0.008	1
Prey length	–6.66	2.97	2.23	0.025	0.8
$Re_{feeding}$	0.04	0.016	2.11	0.034	0.9
$Re_{swimming}$	0.004	0.002	1.75	0.080	0.89
Strike initiation distance	–2.78	1.80	1.54	0.124	0.56
Prey speed	–0.095	0.080	1.18	0.238	0.43

R^2 for these models ranged from 0.54 to 0.59; s.e., adjusted standard error of the estimate. Rank is the relative importance of each term, calculated as a sum of the Akaike weights over all of the models in which the term appears. *N*=100 strikes.

Journal of Experimental Biology (2019) 222, jeb204834. doi:10.1242/jeb.204834

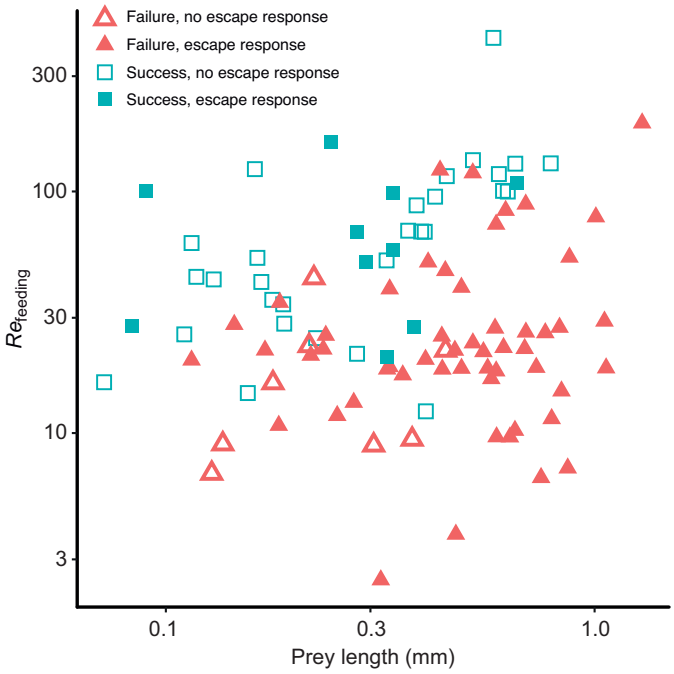

Fig. 3. Prey capture success by larval *S. aurata* increased with increasing *Re* numbers and decreased for larger prey that executed an escape response. $Re_{feeding}$ refers to the *Re* calculated based on mouth diameter and estimated suction flow speed (Eqn 1). Open symbols denote strikes in which the prey did not escape, and filled symbols denote strikes in which the prey executed an escape response. Red triangles indicate larval failure to capture their prey, green squares indicate success. Both *x*- and *y*-axes are plotted on a logarithmic scale. *N*=100 strikes. See also Table 2.

Strike success

A model selection procedure identified seven models that best predict strike outcome based on the independent variables (Table 2). The R^2 for the models ranged from 0.54 to 0.59. An averaging procedure on the selected models revealed that the probability of prey capture increased significantly when prey did not attempt an escape response, when prey length was smaller and when $Re_{feeding}$ was higher (all $P<0.05$; Table 2; Fig. 3). This procedure also provides the relative importance values of each term, calculated as a sum of the Akaike weights over all of the models in which the term appears. The absence of an escape response was the most important predictor of strike success (relative rank=1), followed by $Re_{feeding}$ (0.9), $Re_{swimming}$ (0.89), prey length (0.8), strike initiation distance (0.56) and prey swimming speed (0.43). A linear regression analysis revealed that in successful strikes, prey size increased with larval size ($P<0.002$, $R^2=0.25$).

Table 3. Logistic regression model depicting the effect of the independent variable on prey escape response

	Estimate	s.e.	*Z* value	*P*
Intercept	−0.43	0.90	−0.47	0.63
Prey length	2.50	1.73	1.44	0.14
Larval speed	−0.04	0.01	−4.46	<0.001
Head radius	0.32	2.78	0.11	0.91
Strike initiation distance	3.24	1.18	2.74	0.006

Model $R^2=0.42$; s.e., adjusted standard error of the estimate. *N*=100 strikes.

Prey escape response

Prey escape response was the most important factor in determining feeding success (see above, Movie 1). We therefore used a logistic regression model to test which factors affect the probability of the prey initiating an escape maneuver. The model indicated that increasing larval speed and decreasing strike initiation distance significantly reduced the probability of escape response by the prey ($P<0.006$ for both, $R^2=0.42$; Table 3; Fig. 4), whereas the effects of the other variables were not significant. Thus, the response time available for the prey (strike initiation distance divided by larval speed) was shorter for prey that did not escape (mean±s.e.=0.01±0.0025 s) than for prey that did escape (0.07±0.01 s; Fig. 4B). Additionally, the mean hydrodynamic disturbance (γ, s^{-1}) was lower

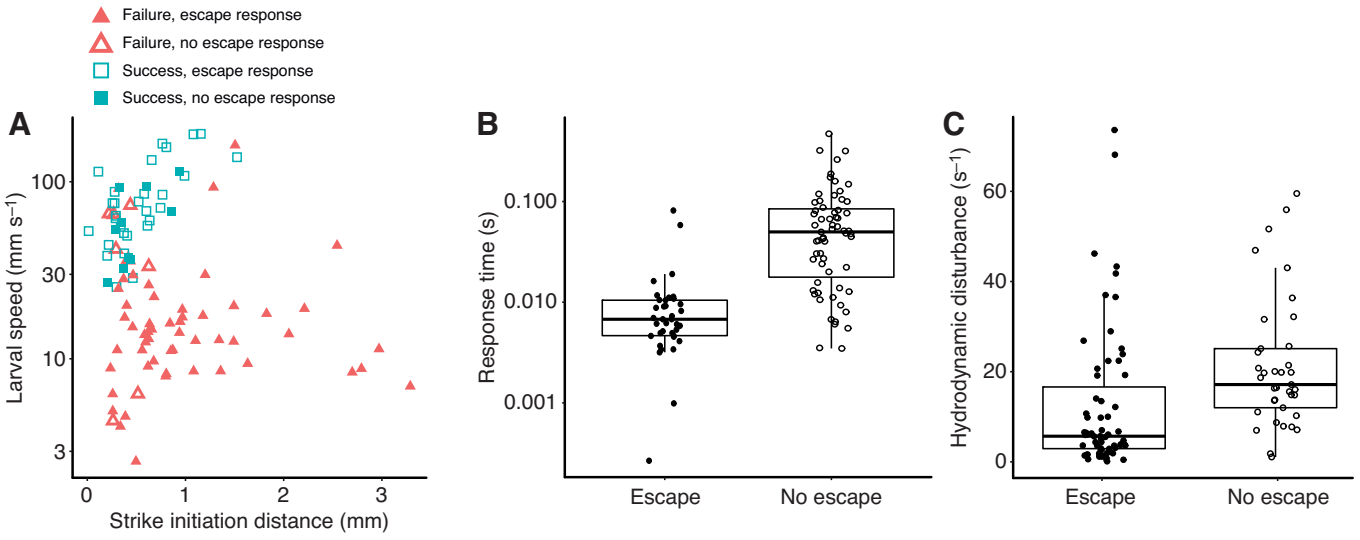

Fig. 4. Prey escape response. (A) The probability of the prey executing an escape response increases at slower larval swimming speeds and in strikes with longer initiation distances (Table 3; *n*=100 strikes). (B) Consequently, the response time available for the prey is shorter for prey that did not attempt an escape maneuver (0.01±0.0025; *n*=37; mean±s.e.) than for prey that attempted to escape (0.07±0.01; *n*=63). (C) The calculated hydrodynamic disturbance (Eqn 2) was higher for prey that did not attempt an escape maneuver (21.2±2.4 s^{-1}) than for prey that executed an escape response (12.3±2.0 s^{-1}). Boxes denote the 1st and 3rd quartiles, black horizontal line is the median, and whiskers denote 1.5 inter-quartile range. Note the logarithmic scale for the *y*-axis in A and B.

for prey that did escape than for prey that did not escape (12.3±2.0 s^{-1} and 21.2±2.4 s^{-1} for escaping and non-escaping prey, respectively; Fig. 4C).

DISCUSSION

In this study, we characterized the interaction between larval fish and prey present in a natural zooplankton assembly dominated by evasive prey. Larvae showed a strong selectivity for large prey that were moving prior to initialization the larva's strike (Fig. 2). As previously shown in studies with non-evasive prey, we found that larval feeding success increased with increasing Reynolds numbers (Fig. 3). However, larval feeding success was also strongly dependent on the prey's escape response (Table 2). Feeding success was lower for larger, more evasive prey (Fig. 3), indicating that larvae might be challenged in capturing their preferred prey. The kinematics of strikes on escaping prey were characterized by slower larval swimming speed and greater strike initiation distance compared with strikes on non-escaping prey (Fig. 4; Table 3). These kinematics resulted in shorter response time and higher hydrodynamic disturbance for prey that did not escape (Fig. 4).

In general, fishes show strong selectivity for large prey (O'Brien et al., 1976; Gardner, 1981; Li et al., 1985; Holzman and Genin, 2003, 2005). Werner and Hall (1974) suggested that such size selection is related to the optimal allocation of time spent searching and handling prey. In contrast to adult fish, larvae are considered selective for smaller, less evasive prey, at least in the first few days after exogeneous feeding begins (Pepin and Penney, 1997; Sabatés and Saiz, 2000; Fulford et al., 2006; Jackson and Lenz, 2016). It is nevertheless unclear why selectivity for small prey might be optimal for larvae. Studies on larval fish selectivity, however, have been largely based on assessing the depletion of prey within an experimental container, or on a comparison between the prey found within the guts of larvae and those in the environment. Either way, such studies integrate two processes within the predator–prey interaction: the first being the recognition and approach to the prey; and the second being the strike itself. In the first stage, selectivity can develop following a bias towards a preferred prey or because of a difference in prey detectability, with both resulting in different attempt rates on different prey types (Werner and Hall, 1974; Li et al., 1985; Buskey et al., 1993; Holzman and Genin, 2005). In the second stage, selectivity can develop following a bias in the ability of the predator to capture certain prey types that better escape or defend themselves. While the idea that copepod escape response may affect predator selectivity was suggested previously (Drenner et al., 1978; Buskey, 1994), we are unaware of any attempts to directly test this idea. To the best of our knowledge, our study is the first to visualize prey selectivity as it takes place in fish. Our findings provide novel insights into the relative roles of a predator's innate preference and its performance in determining larval selectivity. We observed that larvae show a strong preference for directing predatory strikes towards larger, moving prey (Fig. 2). However, this preference would not be reflected in their diet, because such prey is more likely to escape (Figs 2 and 3). Thus, the apparent selectivity for smaller prey by younger larvae could be the result of a prey-size-dependent capture success rather than an active preference for smaller prey.

Previous studies of feeding success by larval fish have focused on their interactions with non-evasive prey (Hernández, 2000; Krebs and Turingan, 2003; China and Holzman, 2014; China et al., 2017), although several studies have reported on interactions between copepods and clownfish larvae (Jackson and Lenz, 2016; Robinson et al., 2019; Tuttle et al., 2019). In small marine larvae that hatch from pelagic eggs, the hydrodynamic environment (denoted by *Re*) is the dominant factor that determines larval kinematics and prey capture performance. However, clownfish larvae hatch at a well-developed state following parental care of the eggs and probably dwell in a realm of higher *Re*. It is therefore unclear how their interactions with evasive prey might represent the general case of all marine larvae. Consequently, a direct comparison of the predatory strategies of representative larvae from these two life-history strategies is warranted.

In general, the dynamics of predator–prey interactions can change depending on the prey's escape response. A numerical model of larval suction flows revealed that smaller (younger) larvae would be able to capture only weakly evasive prey that are attacked from a short distance (relative to the larvae's mouth diameter; Yaniv et al., 2014). The predictions produced by that numerical model for inert prey were the opposite: that the distance within which such prey could be captured would decrease throughout early larval ontogeny (Yaniv et al., 2014). This prediction stems from the change in the spatial pattern of the suction flows that occurs as larvae transition from suction-feeding in a viscous flow regime (*Re* ∼10) at first feeding, to higher *Re* (>100) following settlement (China and Holzman, 2014; Yaniv et al., 2014; China et al., 2017). Suction flows in the intermediate flow environment (*Re* ∼10–30) extend to a distance of ∼2 gape diameters in front of the mouth, whereas at *Re*>100 these flows become more radially symmetric and extend to only ∼1 gape diameter from the mouth (Yaniv et al., 2014; True and Crimaldi, 2017), as also observed in adult fishes (Yaniv et al., 2014; Jacobs and Holzman, 2018). Concomitantly, the force exerted on a prey in the suction flow increases at higher *Re* because of the increase in local and temporal accelerations (Yaniv et al., 2014). Observations on *A. ocellaris* larvae feeding on the calanoid copepod *Bestiolina similis* (Jackson and Lenz, 2016; Tuttle et al., 2019) revealed that feeding success on evasive prey increased throughout ontogeny, and that older larvae are able to capture more evasive prey and from a greater distance compared with younger larvae. The results of the present study (Fig. 4A) further support the CFD prediction (Yaniv et al., 2014), and demonstrate that for interactions with evasive prey, Reynolds number is not the only parameter that determines strike success (Table 2). Specifically, the ability of the prey to execute an escape response at the right time is critically important in determining the outcome of this predator–prey interaction (Table 2). In predator–prey interactions between adult zebrafish and their prey (larval zebrafish), prey that did not initiate an escape response were always captured; whereas escape responses that were timed correctly resulted in prey escape (Stewart et al., 2013). In the present study, prey that did not initiate an escape response were not always captured, probably as a result of the larva's inability to produce a sufficiently strong suction flow. Thus, in larval fish, prey capture is determined on the one hand by the ability of the larva to execute a high *Re* strike and on the other hand by the ability of the prey to execute a timely escape response (Figs 3 and 4).

Copepods are well known for their ability to execute high-acceleration escape responses when sensing a hydrodynamic disturbance (Yen et al., 1992; Fields and Yen, 1997; Buskey et al., 2002; Tuttle et al., 2019). Experiments with siphon flows indicate that copepods escape when exposed to shear rates between 0.5 and 10 s^{-1}, depending on species, developmental stage and previous experience (Viitasalo et al., 1998; Kiørboe and Visser, 1999; Green et al., 2003). Viitasalo et al. (1998) assessed the factors that determine the success of predatory strikes by adult three-spine sticklebacks on two species of copepods. They concluded that feeding success was limited to cases in which the fish was able to approach the copepod slowly. Based on the reaction distance and

fish's speed in cases where the copepod was captured, they inferred that the hydrodynamic signal was weaker than the threshold value of 2.1 and 8.2 s^{-1} that triggered an escape response in their two species (*Eurytemora affinis* and *T. longicornis*, respectively). This 'stealth approach' results in a late escape response and a shorter reaction distance to the approaching predator (Viitasalo et al., 1998). Similar results were observed by Tuttle et al. (2019): the calanoid copepod *B. similis* escaped *A. ocellaris* larvae when exposed to mean water deformation rate higher than 0.37 s^{-1}. In the present study, we found an opposite trend: strike success of *S. aurata* larvae was determined less by stealth (slow approach) and more by brevity. That is, these larvae succeed in capturing copepods by keeping their strikes brief enough to overcome the prey's reaction time and by generating a fast suction flow that exerted stronger suction force on the prey. Similar to sticklebacks, prey capture success was associated with short reaction distances. In *S. aurata* larvae, the strike kinematics on prey that eventually executed an escape response resulted in a longer response time and lower hydrodynamic disturbance available for the prey (Fig. 4). We suggest that this trend might reflect the larvae's inability to correctly time their strike. Striking from too far would allow evasive prey enough time (~70 ms; Fig. 4B) to respond to the hydrodynamic disturbance produced by the predator. Conversely, a stealth approach followed by a fast lunge might provide the prey with little time (<10 ms) to respond to the predator (Tuttle et al., 2019). Thus, despite being 'noisier', successful strikes on evasive prey might depend on striking fast in order to counter the prey's escape response. It could also be that the predators are able to distinguish weakly evasive prey and alter their kinematics accordingly. Additionally, volumetric measurements of the flow around adult zebrafish indicated that the suction flows can counter the hydrodynamic disturbance generated due to the moving body (Gemmell et al., 2014) and can conceal their approach, but it is not known whether this mechanism also applies to other fish species or to larval fish. Unfortunately, our study could not provide taxonomic identity for the prey, and we were not able to relate their response to species identity; future studies should attempt to gain such information.

Acknowledgements
The authors thank N. Paz for editorial assistance, and T. Prevolotsky, C. Jacobs, I. Kolesnikov, T. Gurevich and L. Levi for help with field work.

Competing interests
The authors declare no competing or financial interests.

Author contributions
Conceptualization: N.S., R.H.; Methodology: N.S., R.H.; Validation: N.S., R.H.; Formal analysis: N.S., R.H.; Investigation: N.S.; Resources: R.H.; Data curation: N.S.; Writing - original draft: N.S., R.H.; Writing - review & editing: N.S., R.H.; Visualization: N.S.; Supervision: R.H.; Project administration: R.H.; Funding acquisition: R.H.

Funding
The study was funded by the Israel Science Foundation (965/15 to R.H.). N.S. thanks the Center for Life in Flow (CLiF) for their financial support.

Data availability
Data are available from the Dryad Digital Repository (Sommerfeld and Holzman, 2019): https://doi.org/10.5061/dryad.32qv88r

Supplementary information
Supplementary information available online at
http://jeb.biologists.org/lookup/doi/10.1242/jeb.204834.supplemental

References
Aizaki, H. and Nishimura, K. (2008). Design and analysis of choice experiments using R: a brief introduction. *Agric. Inf. Res.* **17**, 86-94. doi:10.3173/air.17.86

Barneche, D. R., Burgess, S. C. and Marshall, D. J. (2018). Global environmental drivers of marine fish egg size. *Glob. Ecol. Biogeogr.* **27**, 890-898. doi:10.1111/geb.12748

Beaugrand, G., Brander, K. M., Alistair Lindley, J., Souissi, S. and Reid, P. C. (2003). Plankton effect on cod recruitment in the North Sea. *Nature* **426**, 661-664. doi:10.1038/nature02164

Buskey, E. J. (1994). Factors affecting feeding selectivity of visual predators on the copepod *Acartia tonsa*: locomotion, visibility and escape responses. In *Ecology and Morphology of Copepods*, pp. 447-453. Dordrecht, Netherlands: Springer.

Buskey, E. J. and Hartline, D. K. (2003). High-speed video analysis of the escape responses of the copepod *Acartia tonsa* to shadows. *Biol. Bull.* **204**, 28-37. doi:10.2307/1543493

Buskey, E. J., Coulter, C. and Strom, S. (1993). Locomotory patterns of microzooplankton: potential effects on food selectivity of larval fish. *Bull. Mar. Sci.* **53**, 29-43.

Buskey, E. J., Lenz, P. H. and Hartline, D. K. (2002). Escape behavior of planktonic copepods in response to hydrodynamic disturbances: high speed video analysis. *Mar. Ecol. Prog. Ser.* **235**, 135-146. doi:10.3354/meps235135

China, V. and Holzman, R. (2014). Hydrodynamic starvation in first-feeding larval fishes. *Proc. Natl. Acad. Sci. USA* **111**, 8083-8088. doi:10.1073/pnas.1323205111

China, V., Levy, L., Liberzon, A., Elmaliach, T. and Holzman, R. (2017). Hydrodynamic regime determines the feeding success of larval fish through the modulation of strike kinematics. *Proc. R. Soc. B* **284**, 0235 doi:10.1098/rspb.2017.0235

Cowen, R. K. and Sponaugle, S. (2009). Larval dispersal and marine population connectivity. *Annu. Rev. Mar. Sci* **1**, 443-466. doi:10.1146/annurev.marine.010908.163757

Dishon, G., Dubinsky, Z., Fine, M. and Iluz, D. (2012). Underwater light field patterns in subtropical coastal waters: a case study from the Gulf of Eilat (Aqaba). *Isr. J. Plant Sci.* **60**, 265-275. doi:10.1560/IJPS.60.1-2.265

Drenner, R. W., Strickler, J. R. and O'Brien, W. J. (1978). Capture probability: the role of zooplankter escape in the selective feeding of planktivorous fish. *J. Fish. Res. Board Can.* **35**, 1370-1373. doi:10.1139/f78-215

Fields, D. M. and Yen, J. (1997). The escape behavior of marine copepods in response to a quantifiable fluid mechanical disturbance. *J. Plankton Res.* **19**, 1289-1304. doi:10.1093/plankt/19.9.1289

Fulford, R. S., Rice, J. A., Miller, T. J., Binkowski, F. P., Dettmers, J. M. and Belonger, B. (2006). Foraging selectivity by larval yellow perch (*Perca flavescens*): implications for understanding recruitment in small and large lakes. *Can. J. Fish. Aquat. Sci.* **63**, 28-42. doi:10.1139/f05-196

Gardner, M. B. (1981). Mechanisms of size selectivity by planktivorous fish: a test of hypotheses. *Ecology* **62**, 571-578. doi:10.2307/1937723

Gemmell, B. J., Adhikari, D. and Longmire, E. K. (2014). Volumetric quantification of fluid flow reveals fish's use of hydrodynamic stealth to capture evasive prey. *J. R. Soc. Interface* **11**, 20130880. doi:10.1098/rsif.2013.0880

Green, S., Visser, A. W., Titelman, J. and Kiørboe, T. (2003). Escape responses of copepod nauplii in the flow field of the blue mussel, *Mytilus edulis*. *Mar. Biol.* **142**, 727-733. doi:10.1007/s00227-002-0996-1

Hedrick, T. L. (2008). Software techniques for two- and three-dimensional kinematic measurements of biological and biomimetic systems. *Bioinspir. Biomim.* **3**, 034001. doi:10.1088/1748-3182/3/3/034001

Hernández, L. P. (2000). Intraspecific scaling of feeding mechanics in an ontogenetic series of zebrafish, *Danio rerio*. *J. Exp. Biol.* **203**, 3033-3043.

Hjort, J. (1914). Fluctuations in the great fisheries of northern Europe. *Rapp. Pa-V. Reun. Cons. Perm. Int. Explor. Mer* **19**, 1-228.

Holzman, R. and Genin, A. (2003). Zooplanktivory by a nocturnal coral-reef fish: effects of light, flow, and prey density. *Limnol. Oceanogr.* **48**, 1367-1375. doi:10.4319/lo.2003.48.4.1367

Holzman, R. and Genin, A. (2005). Mechanisms of selectivity in a nocturnal fish: a lack of active prey choice. *Oecologia* **146**, 329-336. doi:10.1007/s00442-005-0205-2

Holzman, R., China, V., Yaniv, S. and Zilka, M. (2015). Hydrodynamic constraints of suction feeding in low reynolds numbers, and the critical period of larval fishes. *Integr. Comp. Biol.* **55**, 48-61. doi:10.1093/icb/icv030

Houde, E. D. (1987). Fish early life dynamics and recruitment variability. In American Fisheries Society Symposium, Vol. 2, pp. 17-29.

Houde, E. D. (2008). Emerging from Hjort's shadow. *J. Northwest Atl. Fish. Sci.* **41**, 53-70. doi:10.2960/J.v41.m634

Hunter, J. R. (1981). Feeding ecology and predation of marine fish larvae. In *Marine Fish Larvae* (ed. R. Lasker), pp. 33-79. Seattle: University of Washington Press.

Jackson, J. M. and Lenz, P. H. (2016). Predator-prey interactions in the plankton: larval fish feeding on evasive copepods. *Sci. Rep.* **6**, 33585. doi:10.1038/srep33585

Jacobs, C. N. and Holzman, R. (2018). Conserved spatio-temporal patterns of suction-feeding flows across aquatic vertebrates: a comparative flow visualization study. *J. Exp. Biol.* **221**, jeb174912. doi:10.1242/jeb.174912

Kavanagh, K. D. and Alford, R. A. (2003). Sensory and skeletal development and growth in relation to the duration of the embryonic and larval stages in

damselfishes (Pomacentridae). *Biol. J. Linn. Soc.* **80**, 187-206. doi:10.1046/j.1095-8312.2003.00229.x

Kimmerling, N., Zuqert, O., Amitai, G., Gurevich, T., Armoza-Zvuloni, R., Kolesnikov, I., Berenshtein, I., Melamed, S., Gilad, S., Benjamin, S., et al. (2018). Quantitative species-level ecology of reef fish larvae via metabarcoding. *Nat. Ecol. Evol.* **2**, 306-316. doi:10.1038/s41559-017-0413-2

Kiørboe, T. (2008). *A Mechanistic Approach to Plankton Ecology*. Princeton University Press.

Kiørboe, T. and Visser, A. W. (1999). Predator and prey perception in copepods due to hydromechanical signals. *Mar. Ecol. Prog. Ser.* **179**, 81-95. doi:10.3354/meps179081

Koch, L., Shainer, I., Gurevich, T. and Holzman, R. (2018). The expression of *agrp1*, a hypothalamic appetite-stimulating neuropeptide, reveals hydrodynamic-induced starvation in a larval fish. *Integr. Org. Biol.* **1**, oby003. doi:10.1093/iob/oby003

Krebs, J. M. and Turingan, R. G. (2003). Intraspecific variation in gape–prey size relationships and feeding success during early ontogeny in red drum, *Sciaenops ocellatus*. *Environ. Biol. Fishes* **66**, 75-84. doi:10.1023/A:1023290226801

Li, K. T., Wetterer, J. K. and Hairston, N. G. (1985). Fish size, visula resolution, and prey selectivity. *Ecology* **66**, 1729-1735. doi:10.2307/2937368

O'Brien, W. J., Slade, N. A. and Vinyard, G. L. (1976). Apparent size as the determinant of prey selection by bluegill sunfish (*Lepomis Macrochirus*). *Ecology* **57**, 1304-1310. doi:10.2307/1935055

Olivotto, I., Buttino, I., Borroni, M., Piccinetti, C. C., Malzone, M. G. and Carnevali, O. (2008). The use of the Mediterranean calanoid copepod *Centropages typicus* in yellowtail clownfish (*Amphiprion clarkii*) larviculture. *Aquaculture* **284**, 211-216. doi:10.1016/j.aquaculture.2008.07.057

Pepin, P. and Penney, R. W. (1997). Patterns of prey size and taxonomic composition in larval fish: are there general size-dependent models? *J. Fish Biol.* **51**, 84-100. doi:10.1111/j.1095-8649.1997.tb06094.x

Piccinetti, C. C., Tulli, F., Tokle, N. E., Cardinaletti, G. and Olivotto, I. (2014). The use of preserved copepods in sea bream small-scale culture: biometric, biochemical and molecular implications. *Aquac. Nutr.* **20**, 90-100. doi:10.1111/anu.12055

Robinson, H., Strickler, J. R., Henderson, M. J., Hartline, D. K. and Lenz, P. H. (2019). Predation strategies of larval clownfish capturing evasive copepod prey. *Mar. Ecol. Prog. Ser.* **614**, 125-146. doi:10.3354/meps12888

Sabatés, A. and Saiz, E. (2000). Intra- and interspecific variability in prey size and niche breadth of myctophiform fish larvae. *Mar. Ecol. Prog. Ser.* **201**, 261-271. doi:10.3354/meps201261

Sommerfeld, N. and Holzman, R. (2019). Data from: The interaction between suction feeding performance and prey escape response determines feeding success in larval fish. *Dryad Digital Repository* doi:10.5061/dryad.32qv88r

Stewart, W. J., Cardenas, G. S. and Mchenry, M. J. (2013). Zebrafish larvae evade predators by sensing water flow. *J. Exp. Biol.* **216**, 388-398. doi:10.1242/jeb.072751

Strickler, J. R. and Balázsi, G. (2007). Planktonic copepods reacting selectively to hydrodynamic disturbances. *Philos. Trans. R. Soc. Lond. Ser. B Biol. Sci.* **362**, 1947-1958. doi:10.1098/rstb.2007.2080

Titelman, J. (2001). Swimming and escape behavior of copepod nauplii: Implications for predator-prey interactions among copepods. *Mar. Ecol. Prog. Ser.* **213**, 203-213. doi:10.3354/meps213203

True, A. C. and Crimaldi, J. P. (2017). Hydrodynamics of viscous inhalant flows. *Phys. Rev. E* **95**, 053107. doi:10.1103/PhysRevE.95.053107

Tuttle, L. J., Robinson, H. E., Takagi, D., Strickler, J. R., Lenz, P. H. and Hartline, D. K. (2019). Going with the flow: hydrodynamic cues trigger directed escapes from a stalking predator. *J. R. Soc. Interface* **16**, 20180776. doi:10.1098/rsif.2018.0776

Viitasalo, M., Kiørboe, T., Flinkman, J., Pedersen, L. W. and Visser, A. W. (1998). Predation vulnerability of planktonic copepods: Consequences of predator foraging strategies and prey sensory abilities. *Mar. Ecol. Prog. Ser.* **175**, 129-142. doi:10.3354/meps175129

Vogel, S. (1994). *Life in Moving Fluids: the Physical Biology of Flow*, 2nd edn. Princeton University Press.

Vonta, I. (2010). Model selection and model averaging. *J. Appl. Stat.* **37**, 1419-1420. doi:10.1080/02664760902899774

Werner, E. E. and Hall, D. J. (1974). Optimal foraging and the size selection of prey by the bluegill sunfish (*Lepomis macrochirus*). *Ecology* **55**, 1042-1052. doi:10.2307/1940354

Yaniv, S., Elad, D. and Holzman, R. (2014). Suction feeding across fish life stages: flow dynamics from larvae to adults and implications for prey capture. *J. Exp. Biol.* **217**, 3748-3757. doi:10.1242/jeb.104331

Yavno, S. and Holzman, R. (2018). Do viscous forces affect survival of marine fish larvae? Revisiting the 'safe harbour' hypothesis. *Rev. Fish Biol. Fish.* **28**, 201-212. doi:10.1007/s11160-017-9503-0

Yen, J. and Strickler, J. R. (1996). Advertisement and concealment in the plankton: what makes a copepod hydrodynamically conspicuous? *Invertebr. Biol.* **115**, 191-205. doi:10.2307/3226930

Yen, J., Lenz, P. H., Gassie, D. V. and Hartline, D. K. (1992). Mechanoperception in marine copepods: electrophysiological studies on the first antennae. *J. Plankton Res.* **14**, 495-512. doi:10.1093/plankt/14.4.495